PHYS 3038 Optics
L15 Interference
Reading Material: Ch9.4-6

Shengwang Du

2015, the Year of Light

Mirrored Interferometers

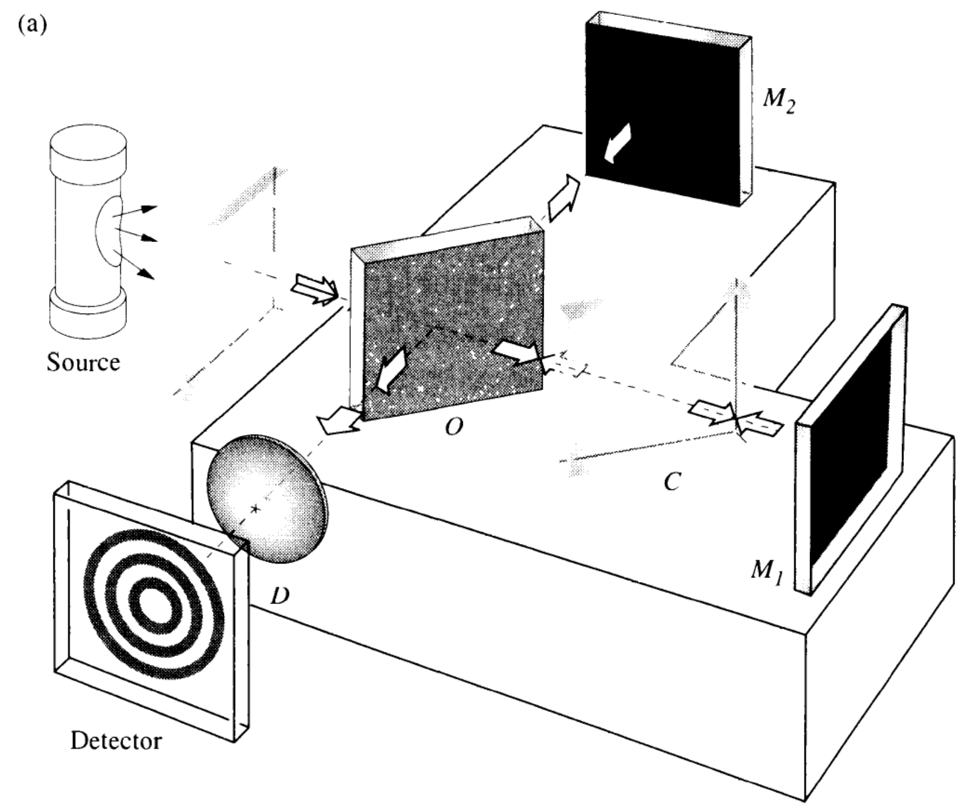

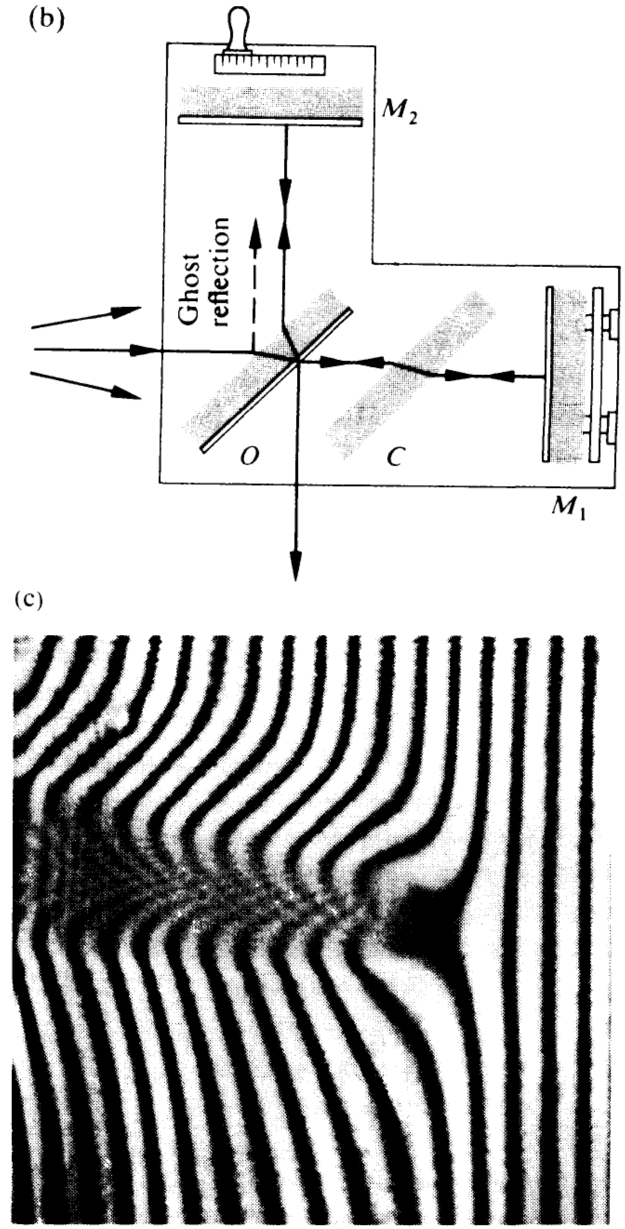

Figure 9.24 The Michelson Interferometer. (*a*) Circular fringes are centered on the lens. (*b*) Top view of the interferometer showing the path of the light. (*c*) A wedge fringe pattern was distorted when the tip of a hot soldering iron was placed in one arm. Observe the interesting perceptual phenomenon whereby the region corresponding to the iron's tip appears faintly yellow. (Photo by E. H.)

Haidenger fringes: equal inclination

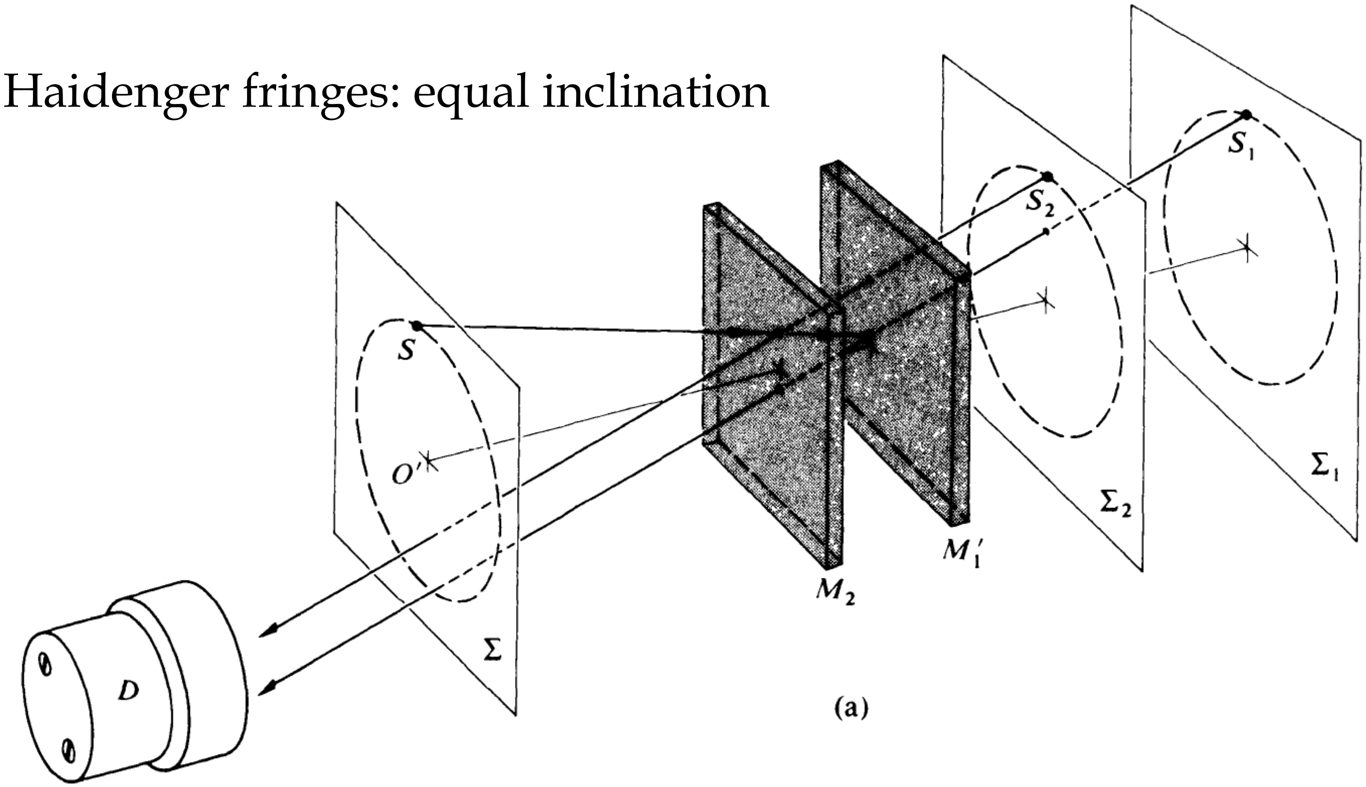

(a)

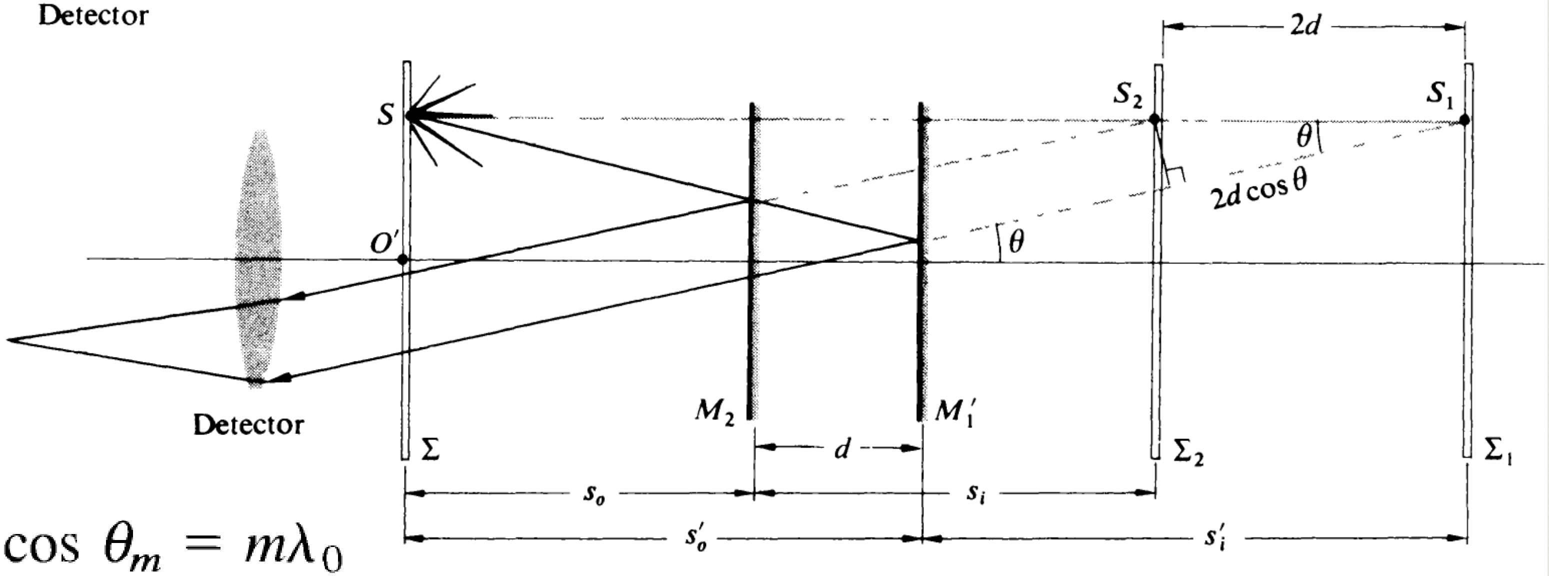

$$2d \cos \theta_m = m\lambda_0$$

(b)

Michelson Interferometer

$$2d \cos \theta_m = m\lambda_0$$

For fixed θ=0

$$2d = m\lambda_0$$
$$d = m(\lambda_0/2)$$

$$\Delta d = \Delta m(\lambda_0/2) = N(\lambda_0/2)$$

Mach-Zehnder Interferometer

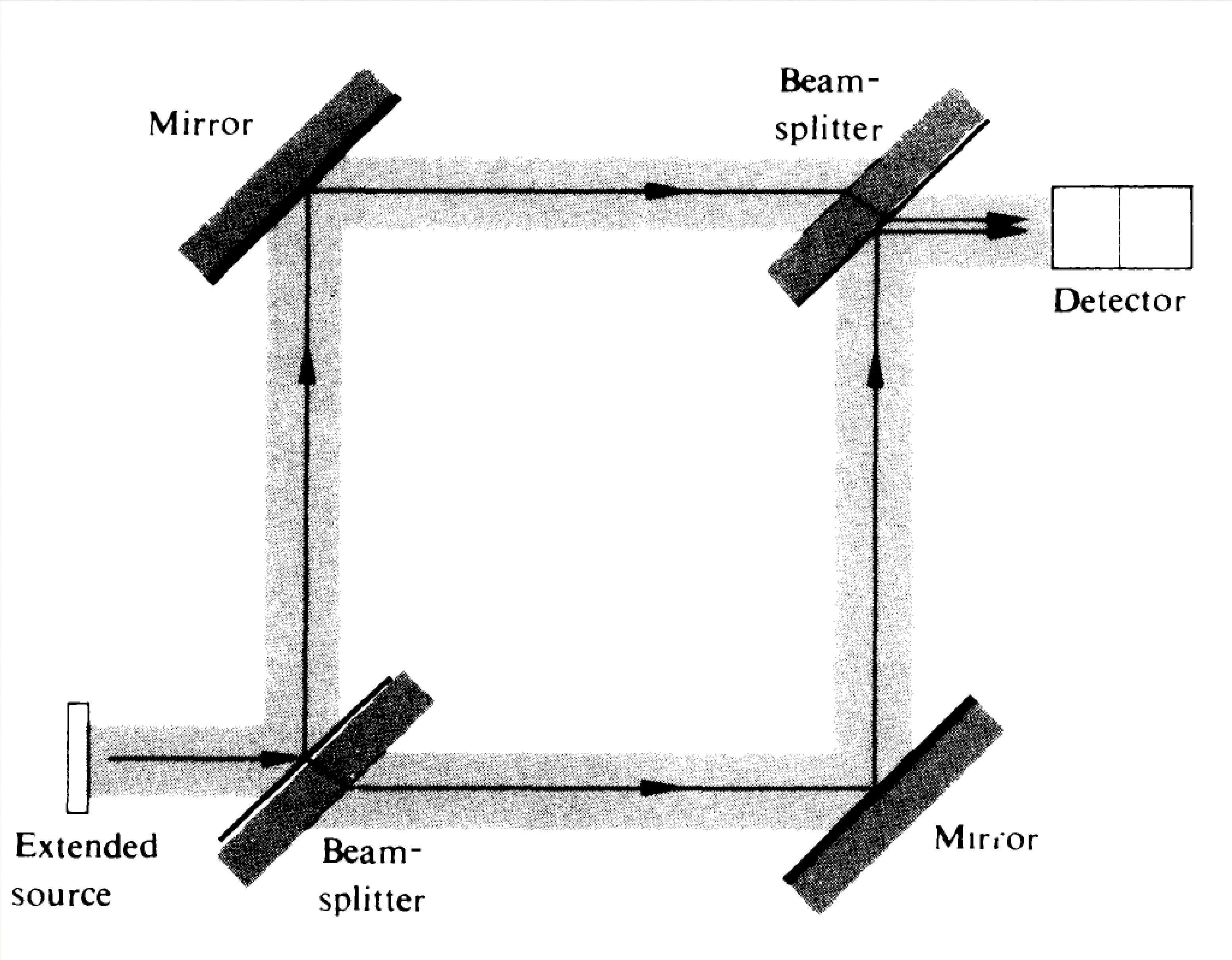

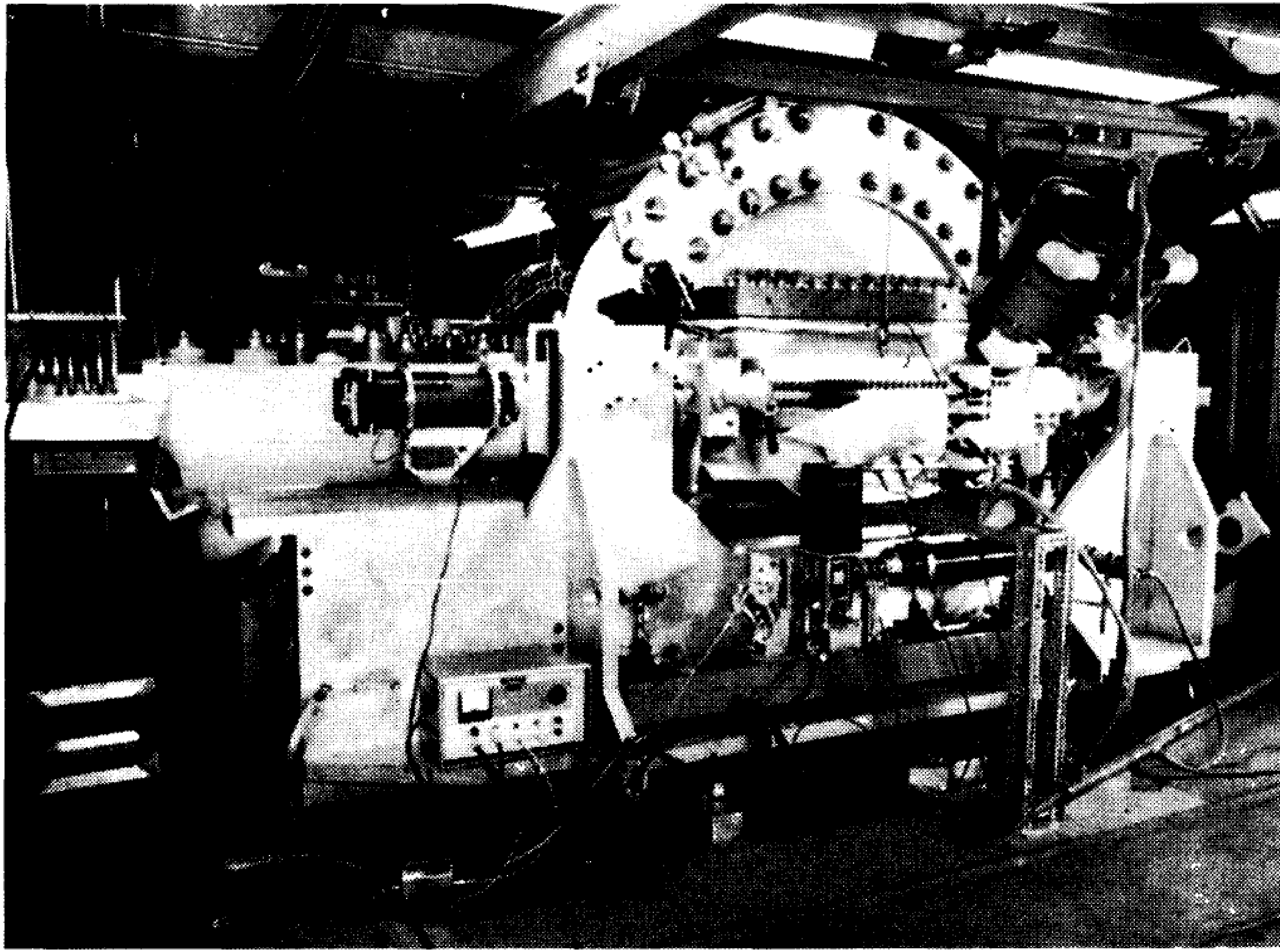

Scylla IV, an early setup for studying plasma. (Courtesy of University of California, Lawrence Livermore National Laboratory, and the Department of Energy.)

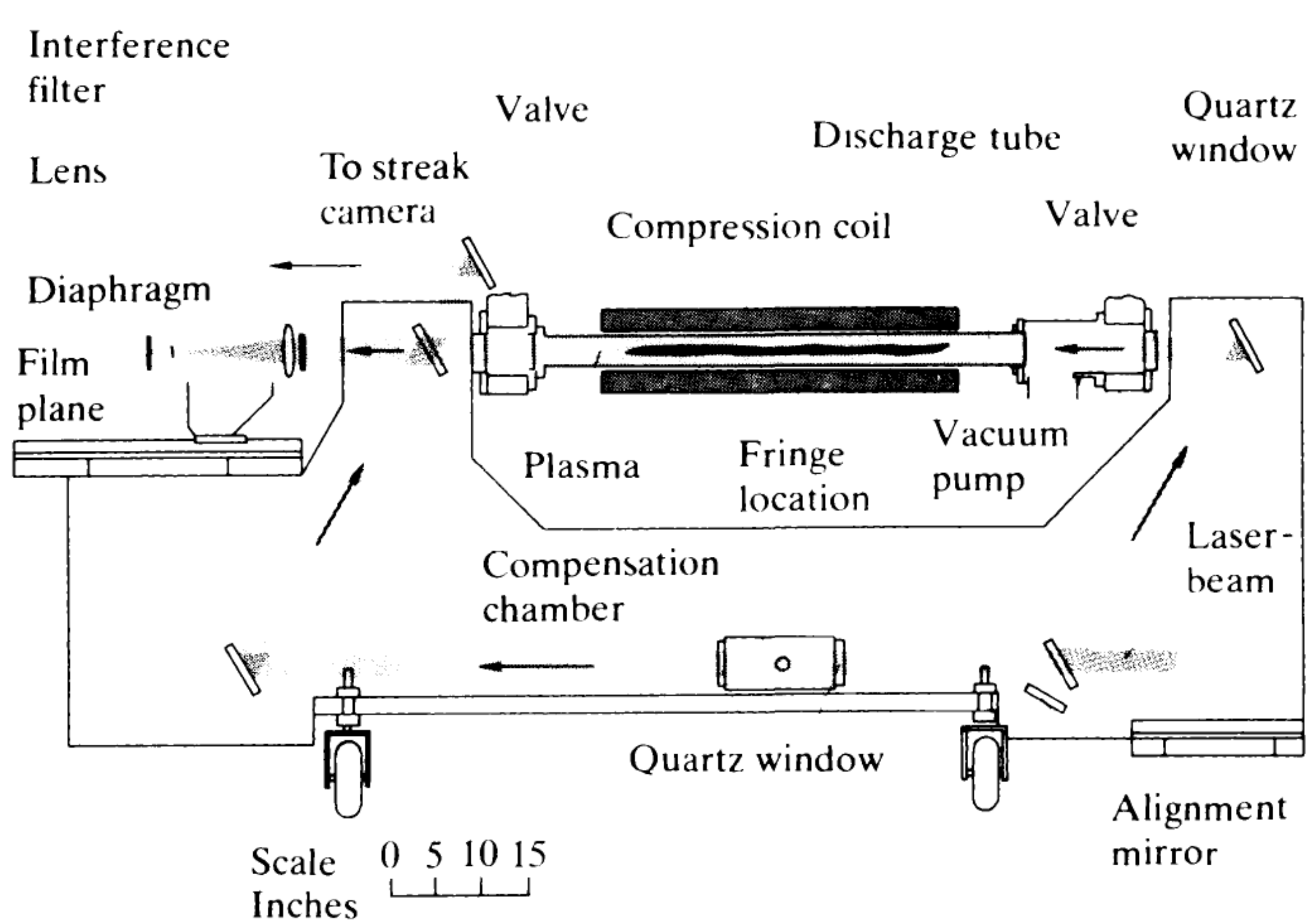

Schematic of Scylla IV.

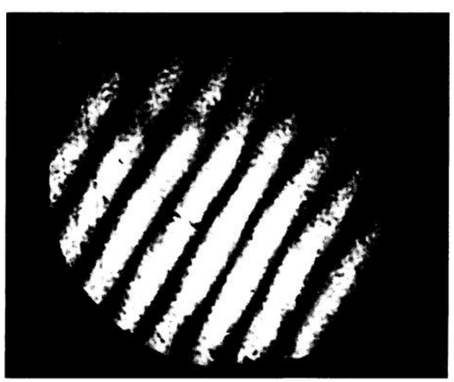

Interferogram without plasma. (Photo courtesy Los Alamos National Laboratory.)

Interferogram with plasma. (Photo courtesy Los Alamos National Laboratory.)

Sagnac Interometer

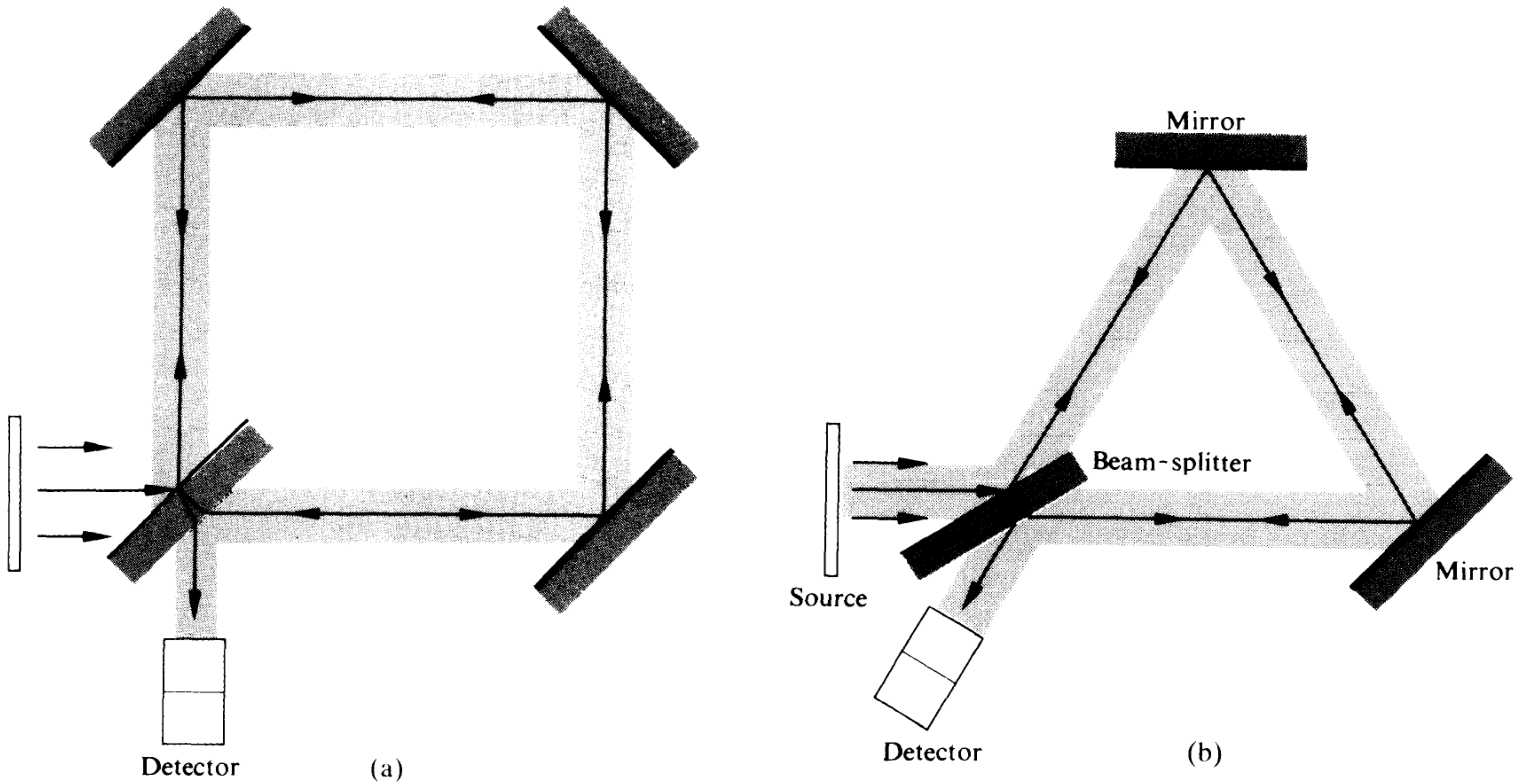

Figure 9.29 (***a***) A Sagnac Interferometer. (***b***) Another variation of the Sagnac Interferometer.

Pohl Interometer

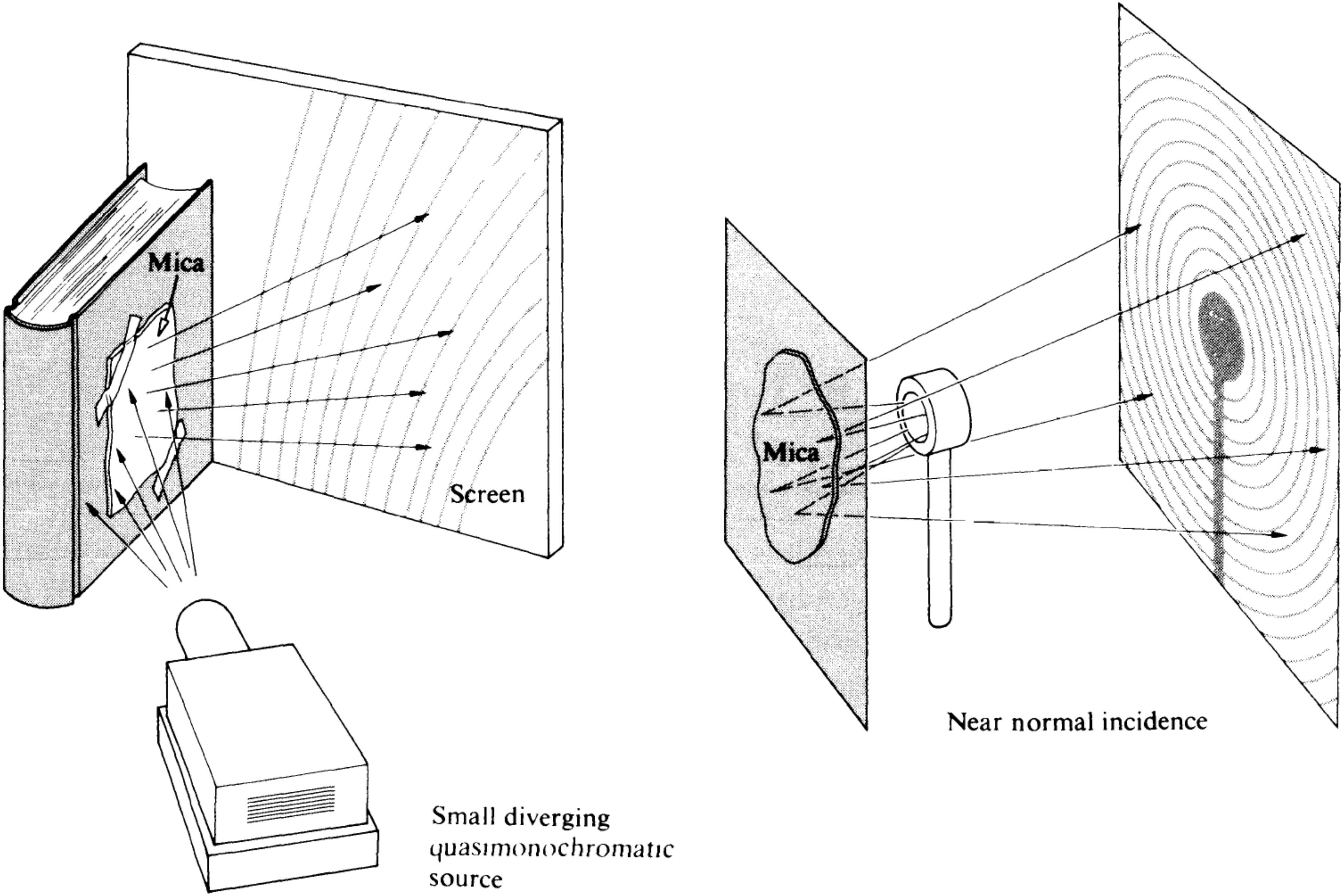

Pohl Interometer

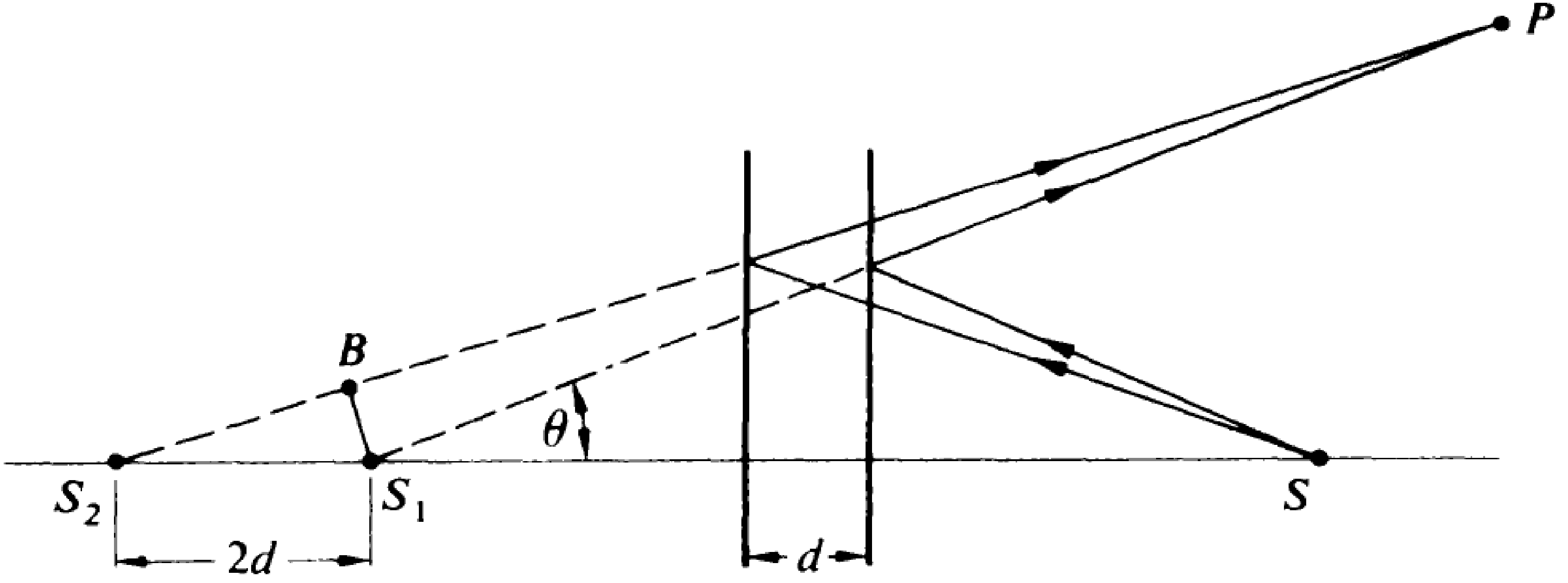

Figure 9.31 Point-source illumination of parallel surfaces.

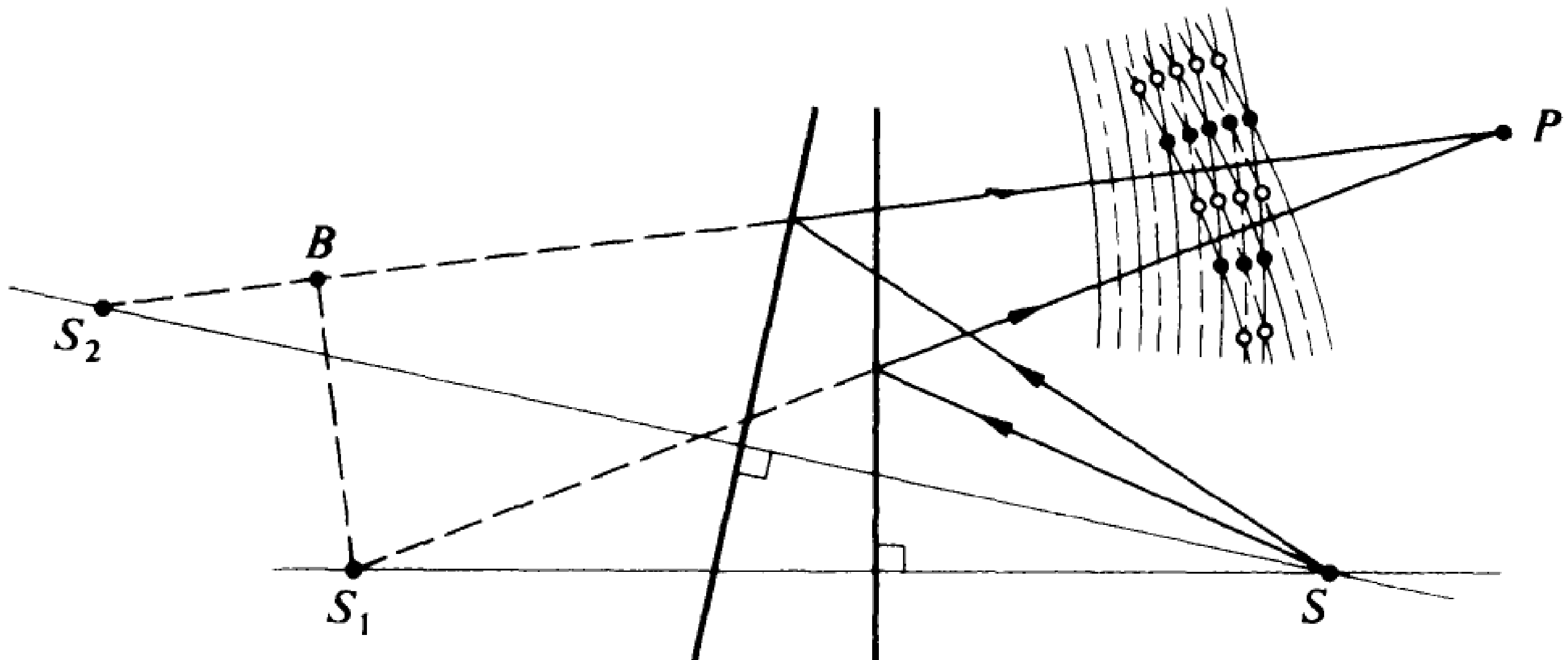

Figure 9.32 Point-source illumination of inclined surfaces.

Types and Localization of Interference Fringes

- Real fringes: can be seen on a screen without the use of additional focusing system.
- Virtunal fringes: cannot be projected onto a screen without a focusing system.
- Nonlocalized fringes: 3D (from a point or line source)
- Localized fringes: observable only over a particular surface (from an extended source)

9.6 Multiple Beam Interference

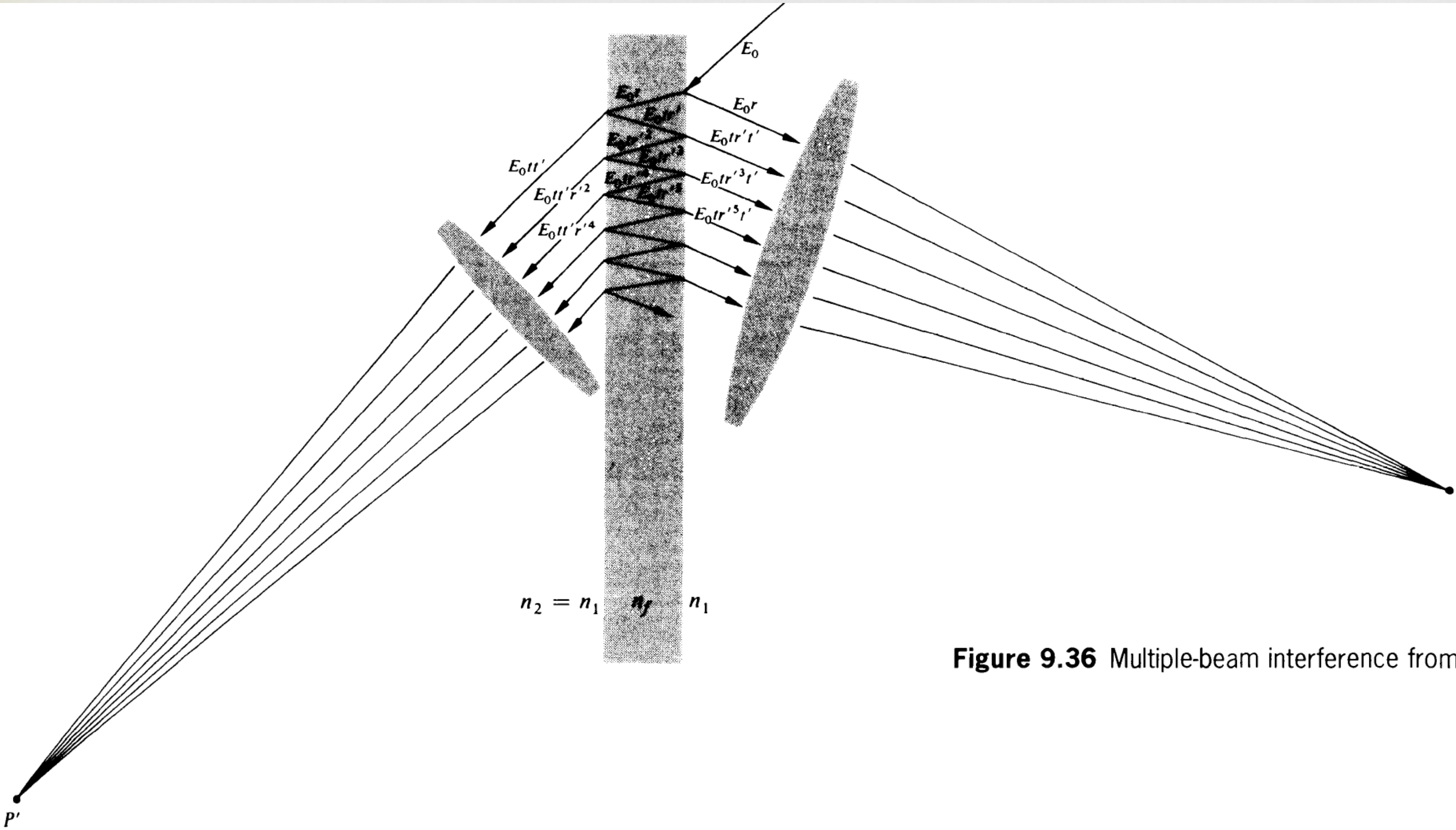

Figure 9.36 Multiple-beam interference from a parallel film.

Amplitude Coefficients

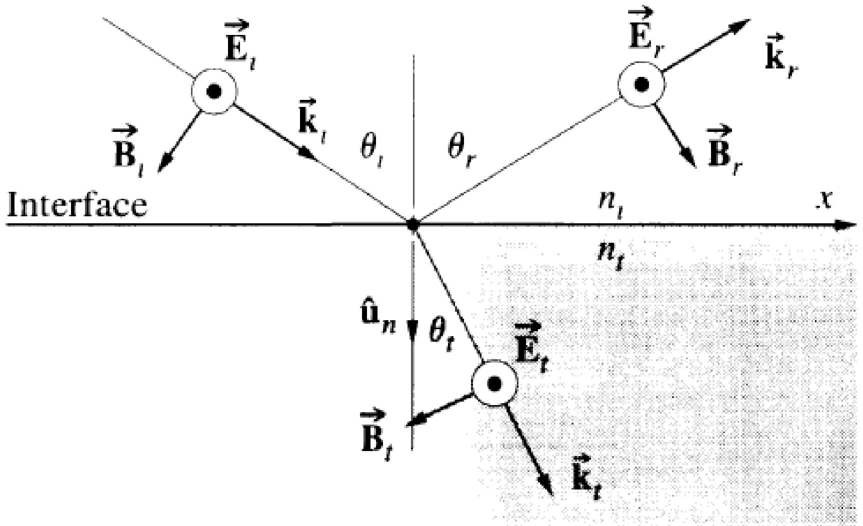

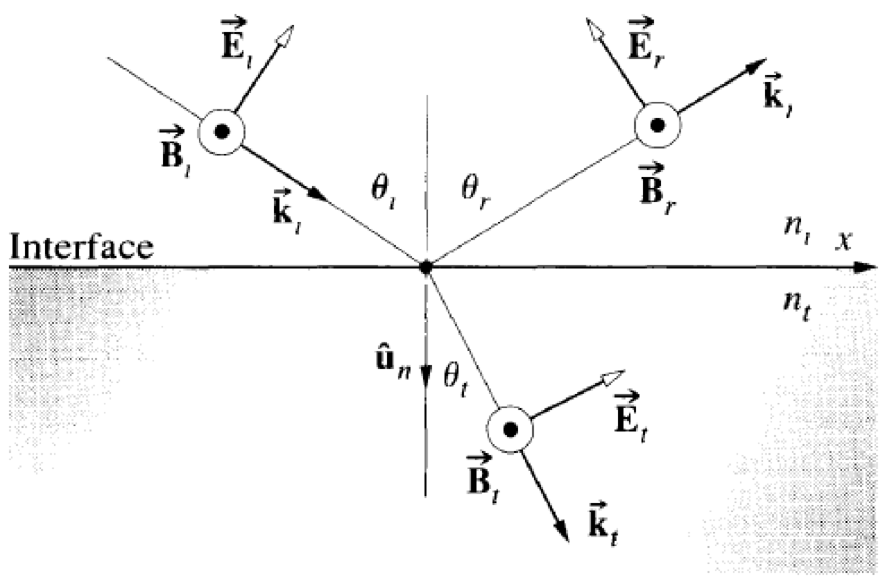

$$r_\perp = -\frac{\sin(\theta_i - \theta_t)}{\sin(\theta_i + \theta_t)} \tag{4.42}$$

$$r_\parallel = +\frac{\tan(\theta_i - \theta_t)}{\tan(\theta_i + \theta_t)} \tag{4.43}$$

$$t_\perp = +\frac{2\sin\theta_t\cos\theta_i}{\sin(\theta_i + \theta_t)} \tag{4.44}$$

$$t_\parallel = +\frac{2\sin\theta_t\cos\theta_i}{\sin(\theta_i + \theta_t)\cos(\theta_i - \theta_t)} \tag{4.45}$$

$\theta_i < \theta_p$

$n_i < n_t$ $\theta_i > \theta_t$

$r_\perp < 0$ $r_{||} > 0$

$n_i > n_t$ $\theta_i < \theta_t$

$r_\perp > 0$ $r_{||} < 0$

Thin Film

$\theta_i < \theta_p$

$\Lambda = 2n_f d \cos\theta_t$

if $\Lambda = m\lambda$,

$$E_{0r} = E_0 r - (E_0 t r t' + E_0 t r^3 t' + E_0 t r^5 t' + \cdots)$$

or

$$E_{0r} = E_0 r - E_0 t r t'(1 + r^2 + r^4 + \cdots)$$

$$E_{0r} = E_0 r - \frac{E_0 t r t'}{(1 - r^2)}$$

$$tt' = 1 - r^2$$

$$E_{0r} = 0$$

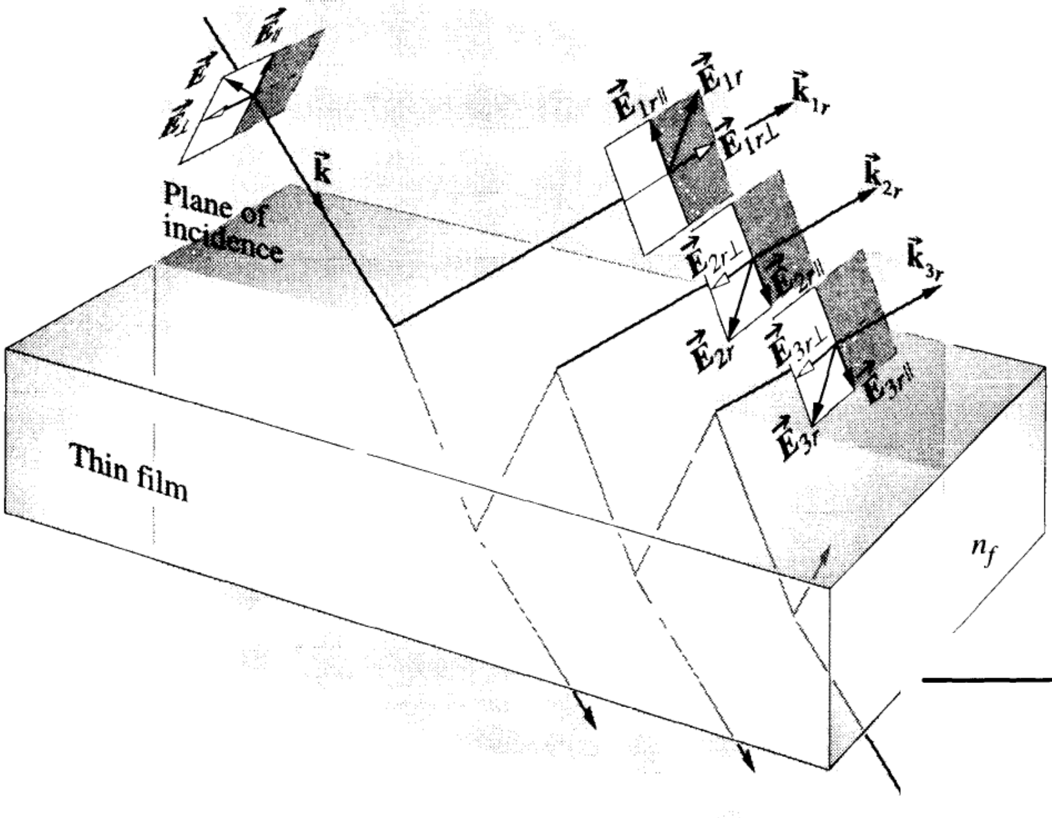

Figure 9.37 Phase shifts arising purely from the reflections (internal $\theta_i < \theta_p'$).

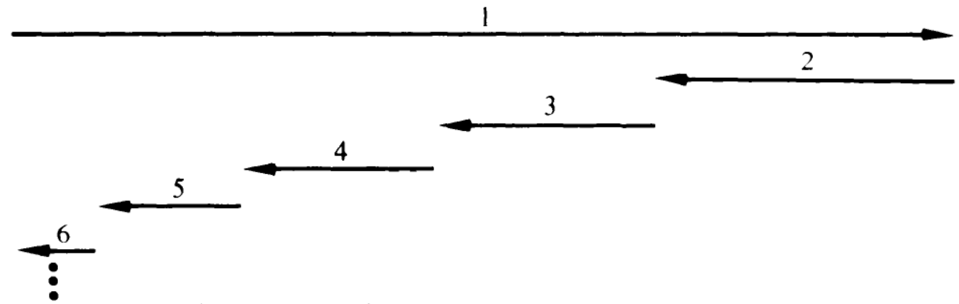

$E_{0r} = 0$ (Resultant amplitude)

Figure 9.38 Phasor diagram.

Maximum Reflection: Thin Film

is transmitted. The *second special case* arises when $\Lambda = (m + \frac{1}{2})\lambda$. Now the first and second rays are in-phase, and all other adjacent waves are $\lambda/2$ out-of-phase; that is, the second is out-of-phase with the third, the third is out-of-phase with the fourth, and so on. The resultant *scalar amplitude* is then

$$E_{0r} = E_0 r + E_0 t r t' - E_0 t r^3 t' + E_0 t r^5 t' - \cdots$$

or

$$E_{0r} = E_0 r + E_0 r t t'(1 - r^2 + r^4 - \cdots)$$

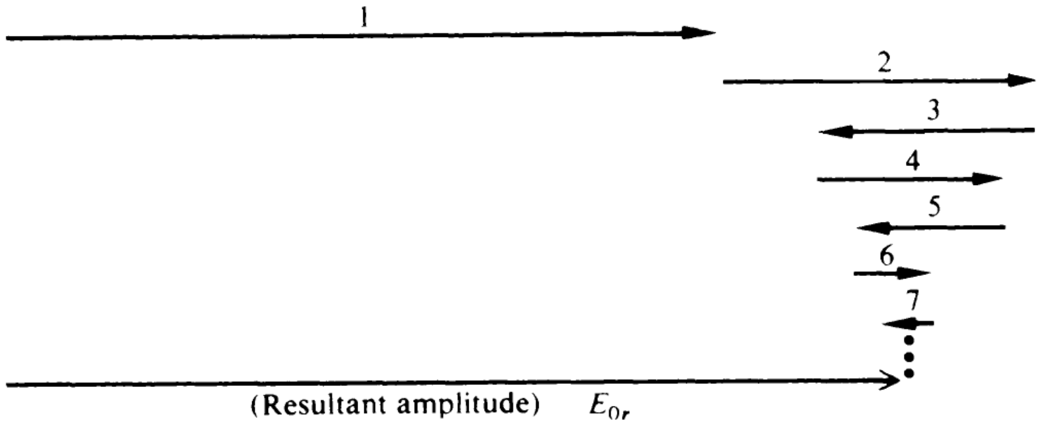

The series in parentheses is equal to $1/(1 + r^2)$, in which case

$$E_{0r} = E_0 r\left[1 + \frac{tt'}{(1 + r^2)}\right]$$

Again, $tt' = 1 - r^2$; therefore, as illustrated in Fig. 9.39,

$$E_{0r} = \frac{2r}{(1 + r^2)} E_0$$

Since this particular arrangement results in the addition of the first and second waves, which have relatively large amplitudes, it should yield a large reflected flux density. The irradiance is proportional to $E_{0r}^2/2$, so from Eq. (3.44)

$$I_r = \frac{4r^2}{(1 + r^2)^2}\left(\frac{E_0^2}{2}\right) \tag{9.50}$$

That this is in fact the maximum, $(I_r)_{\max}$, will be shown later.

General Cas

$n_1 = n_2 \qquad \theta_i < \theta_p$

$$\tilde{E}_{1r} = E_0 r e^{i\omega t}$$

$$\tilde{E}_{2r} = E_0 t r' t' e^{i(\omega t - \delta)}$$

$$\tilde{E}_{3r} = E_0 t r'^3 t' e^{i(\omega t - 2\delta)}$$

$$\vdots$$

$$\tilde{E}_{Nr} = E_0 t r'^{(2N-3)} t' e^{i[\omega t - (N-1)\delta]}$$

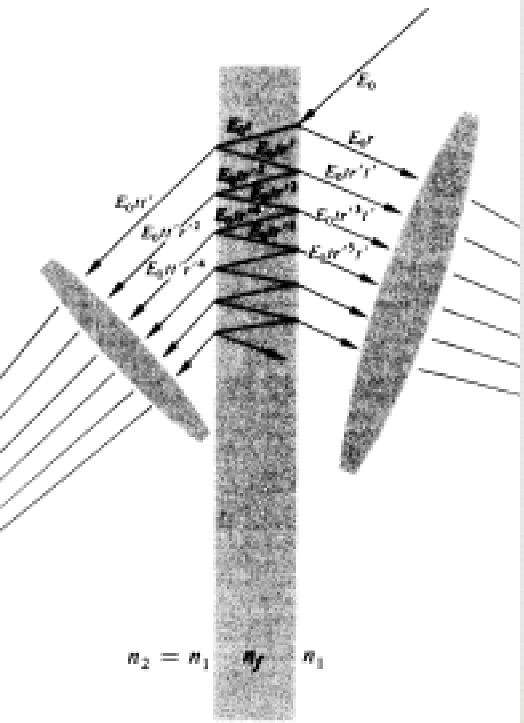

$$\tilde{E}_r = \tilde{E}_{1r} + \tilde{E}_{2r} + \tilde{E}_{3r} + \cdots + \tilde{E}_{Nr}$$

or upon substitution (Fig. 9.40)

$$\tilde{E}_r = E_0 r e^{i\omega t} + E_0 t r' t' e^{i(\omega t - \delta)} + \cdots + E_0 t r'^{(2N-3)} t' \times e^{i[\omega t - (N-1)\delta]}$$

This can be rewritten as

$$\tilde{E}_r = E_0 e^{i\omega t}\{r + r' t t' e^{-i\delta}[1 + (r'^2 e^{-i\delta}) + (r'^2 e^{-i\delta})^2 + \cdots + (r'^2 e^{-i\delta})^{N-2}]\}$$

If $|r'^2 e^{-i\delta}| < 1$, and if the number of terms in the series approaches infinity, the series converges. The resultant wave becomes

$$\tilde{E}_r = E_0 e^{i\omega t}\left[r + \frac{r' t t' e^{-i\delta}}{1 - r'^2 e^{-i\delta}}\right] \qquad (9.51)$$

In the case of zero absorption, no energy being taken out of the waves, we can use the relations $r = -r'$ and $tt' = 1 - r^2$ to rewrite Eq. (9.51) as

$$\tilde{E}_r = E_0 e^{i\omega t}\left[\frac{r(1 - e^{-i\delta})}{1 - r^2 e^{-i\delta}}\right]$$

Phasor diagram

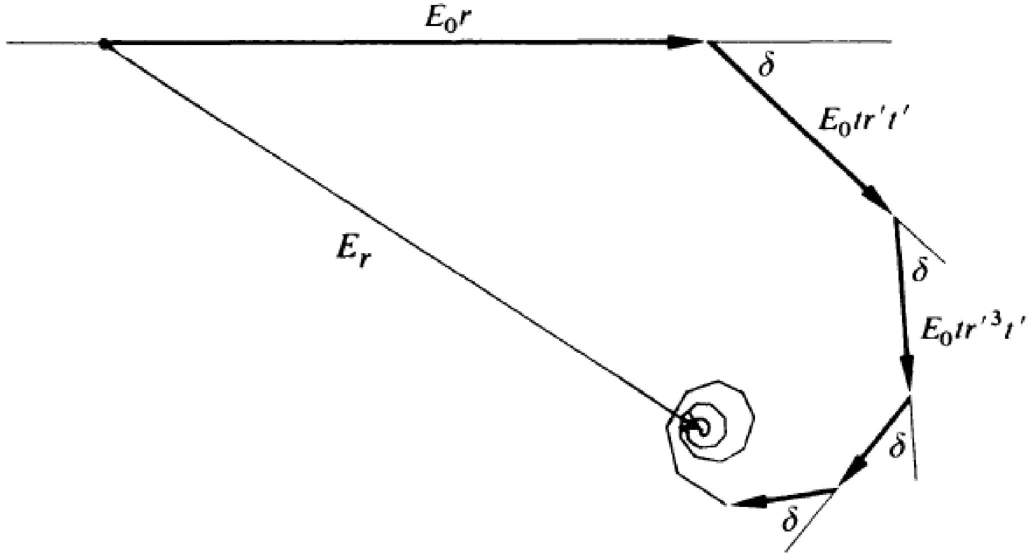

Figure 9.40 Phasor diagram.

The reflected flux density at P is then $I_r = \tilde{E}_r \tilde{E}_r^*/2$, that is,

$$I_r = \frac{E_0^2 r^2 (1 - e^{-i\delta})(1 - e^{+i\delta})}{2(1 - r^2 e^{-i\delta})(1 - r^2 e^{+i\delta})}$$

which can be transformed into

$$I_r = I_i \frac{2r^2(1 - \cos\delta)}{(1 + r^4) - 2r^2 \cos\delta} \qquad (9.52)$$

The symbol $I_i = E_0^2/2$ represents the incident flux density,

Transmission

$n_1 = n_2$

$$\tilde{E}_{1t} = E_0 tt' e^{i\omega t}$$

$$\tilde{E}_{2t} = E_0 tt' r'^2 e^{i(\omega t - \delta)}$$

$$\tilde{E}_{3t} = E_0 tt' r'^4 e^{i(\omega t - 2\delta)}$$

$$\vdots$$

$$\tilde{E}_{Nt} = E_0 tt' r'^{2(N-1)} e^{i[\omega - (N-1)\delta]}$$

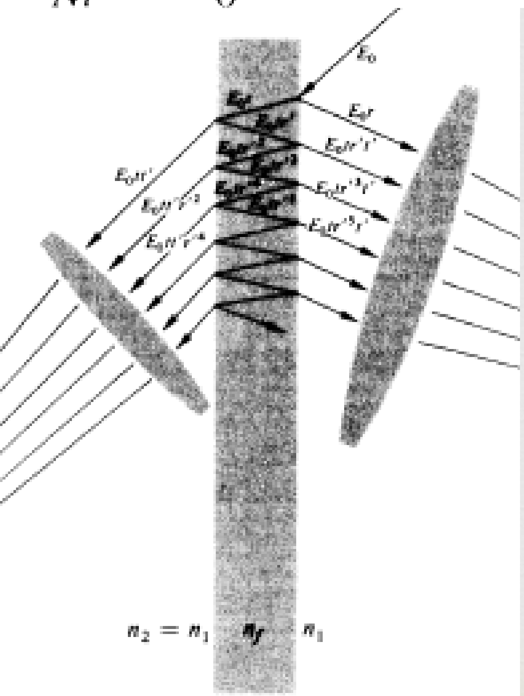

$$\tilde{E}_t = E_0 e^{i\omega t}\left[\frac{tt'}{1 - r^2 e^{-i\delta}}\right]$$

$$I_t = \frac{I_i (tt')^2}{(1 + r^4) - 2r^2 \cos\delta}$$

Multiple Beam Interference

$$I_r = I_i \frac{[2r/(1-r^2)]^2 \sin^2(\delta/2)}{1 + [2r/(1-r^2)]^2 \sin^2(\delta/2)}$$

$$I_t = I_i \frac{1}{1 + [2r/(1-r^2)]^2 \sin^2(\delta/2)}$$

$$I_i = I_r + I_t$$

$$(I_t)_{\max} = I_i$$

$$(I_r)_{\min} = 0$$

$$(I_t)_{\min} = I_i \frac{(1-r^2)^2}{(1+r^2)^2}$$

$$(I_r)_{\max} = I_i \frac{4r^2}{(1+r^2)^2}$$

Multiple Beam Interference

Coefficient of finesse

$$F \equiv \left(\frac{2r}{1 - r^2} \right)^2$$

$$\delta = 2k_f d cos\theta_t = \frac{4\pi n_f}{\lambda_0} \mathrm{d} \cos\theta_t$$

$$\frac{I_r}{I_i} = \frac{F \sin^2 (\delta/2)}{1 + F \sin^2(\delta/2)}$$

$$\frac{I_t}{I_i} = \frac{1}{1 + F \sin^2(\delta/2)}$$

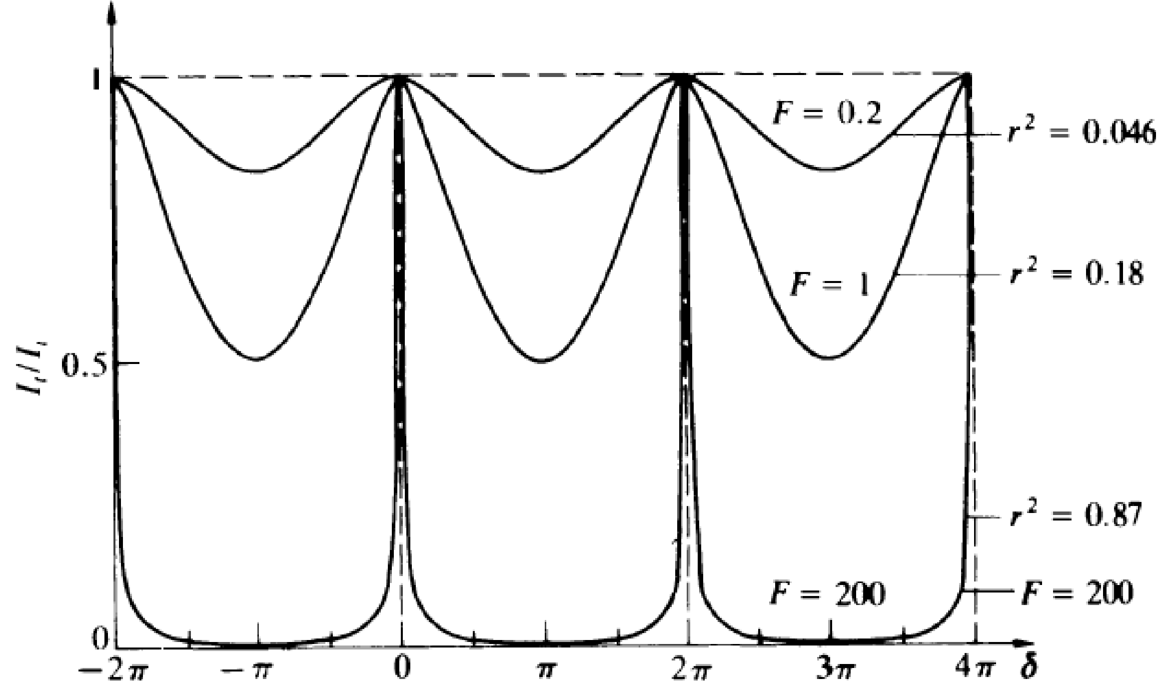

1
0.5
0
I_t/I_i
F = 0.2
$r^2 = 0.046$
F = 1
$r^2 = 0.18$
$r^2 = 0.87$
F = 200
F = 200
-2π
$-\pi$
0
π
2π
3π
4π
δ

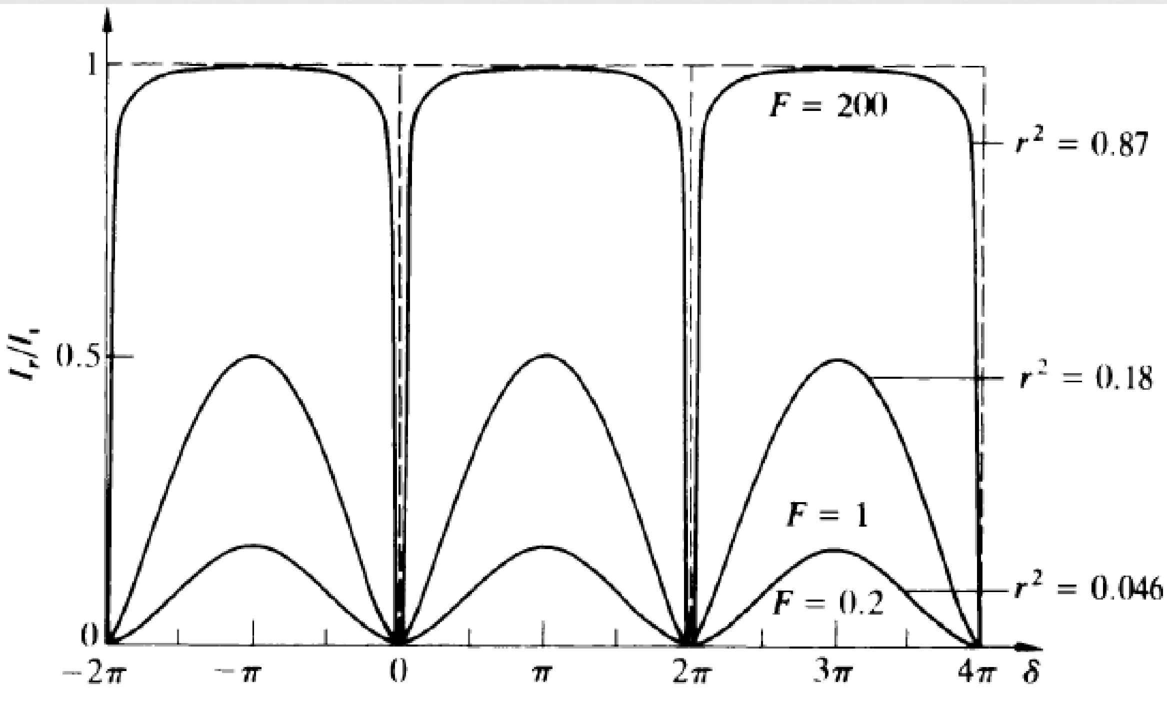

1
0.5
0
I_r/I_i
F = 200
$r^2 = 0.87$
$r^2 = 0.18$
F = 1
F = 0.2
$r^2 = 0.046$
-2π
$-\pi$
0
π
2π
3π
4π
δ

Fabry-Perot Interferometer

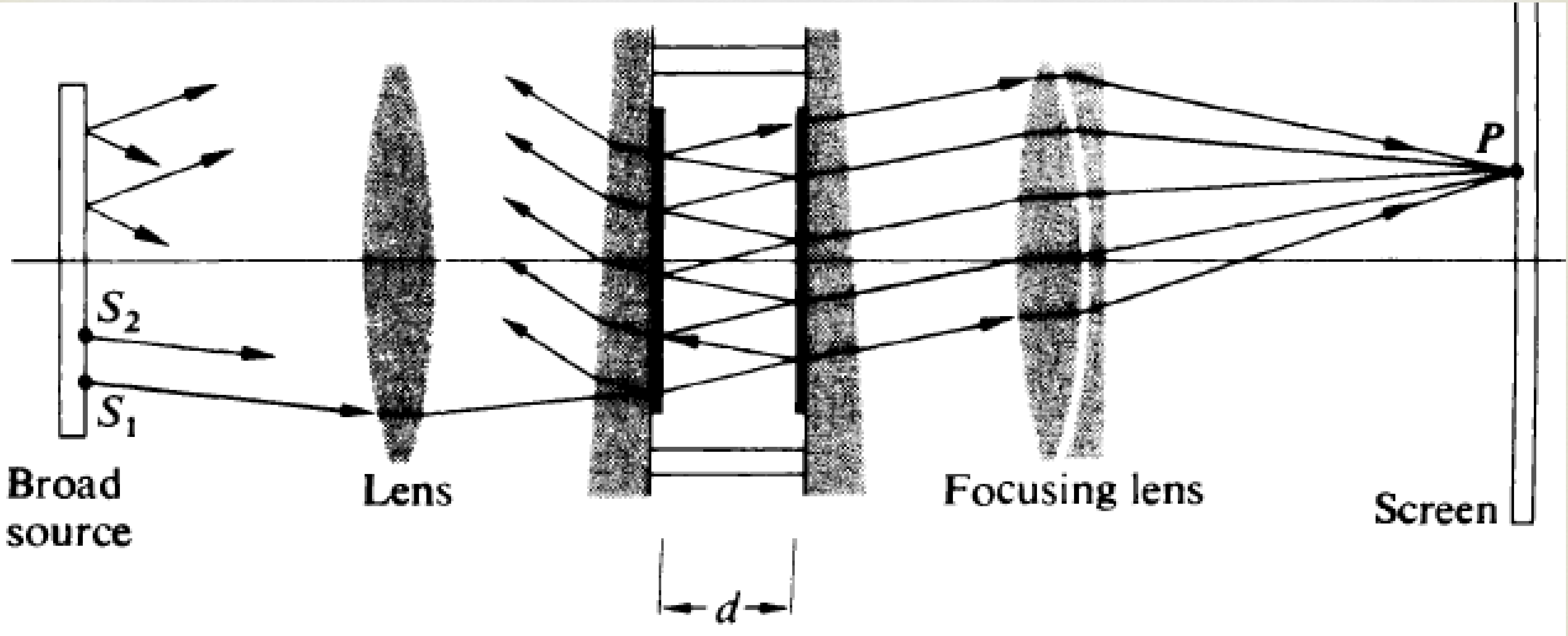

Figure 9.43 Fabry–Perot etalon.

Fabry-Perot Interferometer

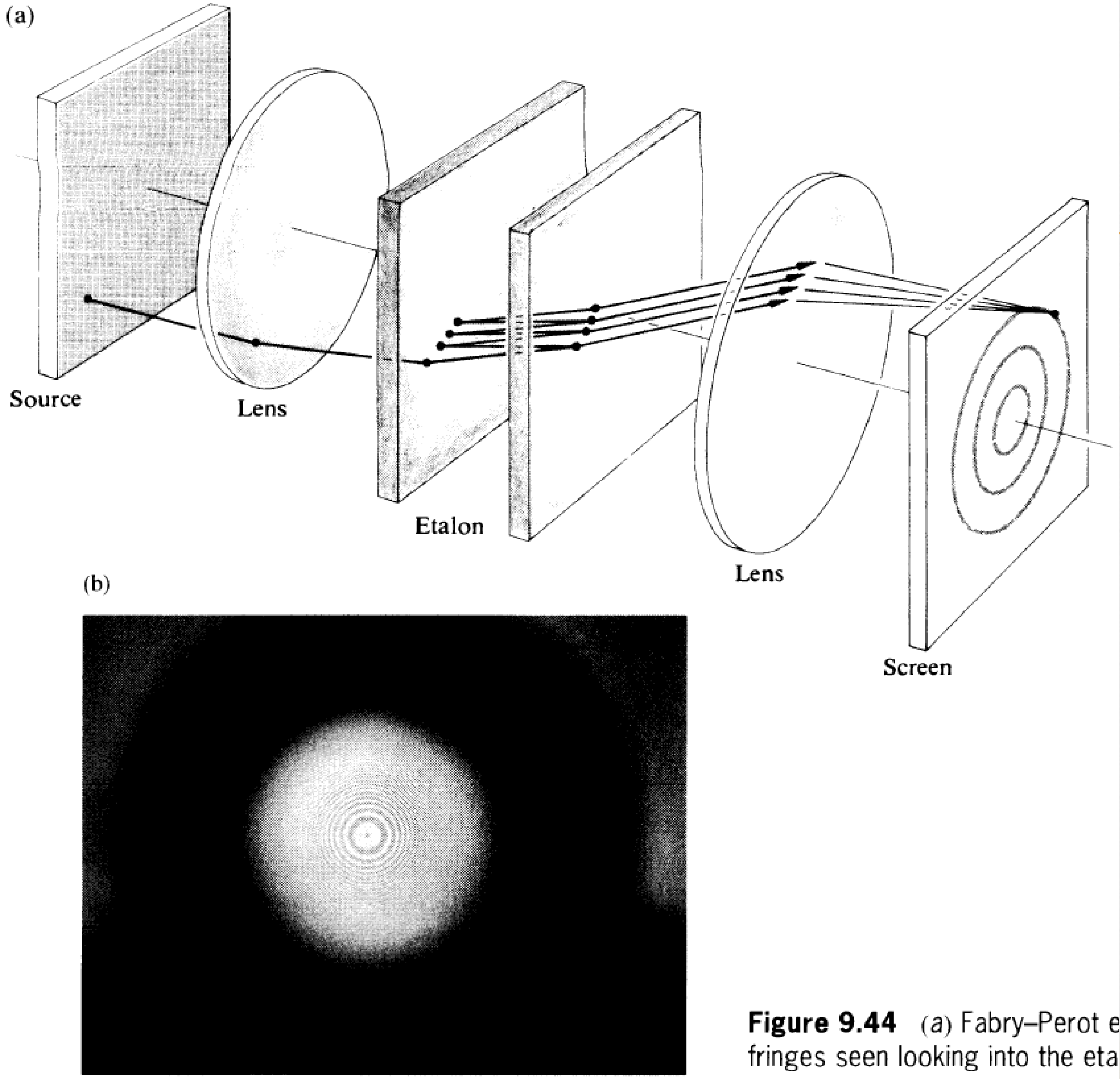

Figure 9.44 (*a*) Fabry–Perot e
fringes seen looking into the eta

Fabry-Perot Interferometer

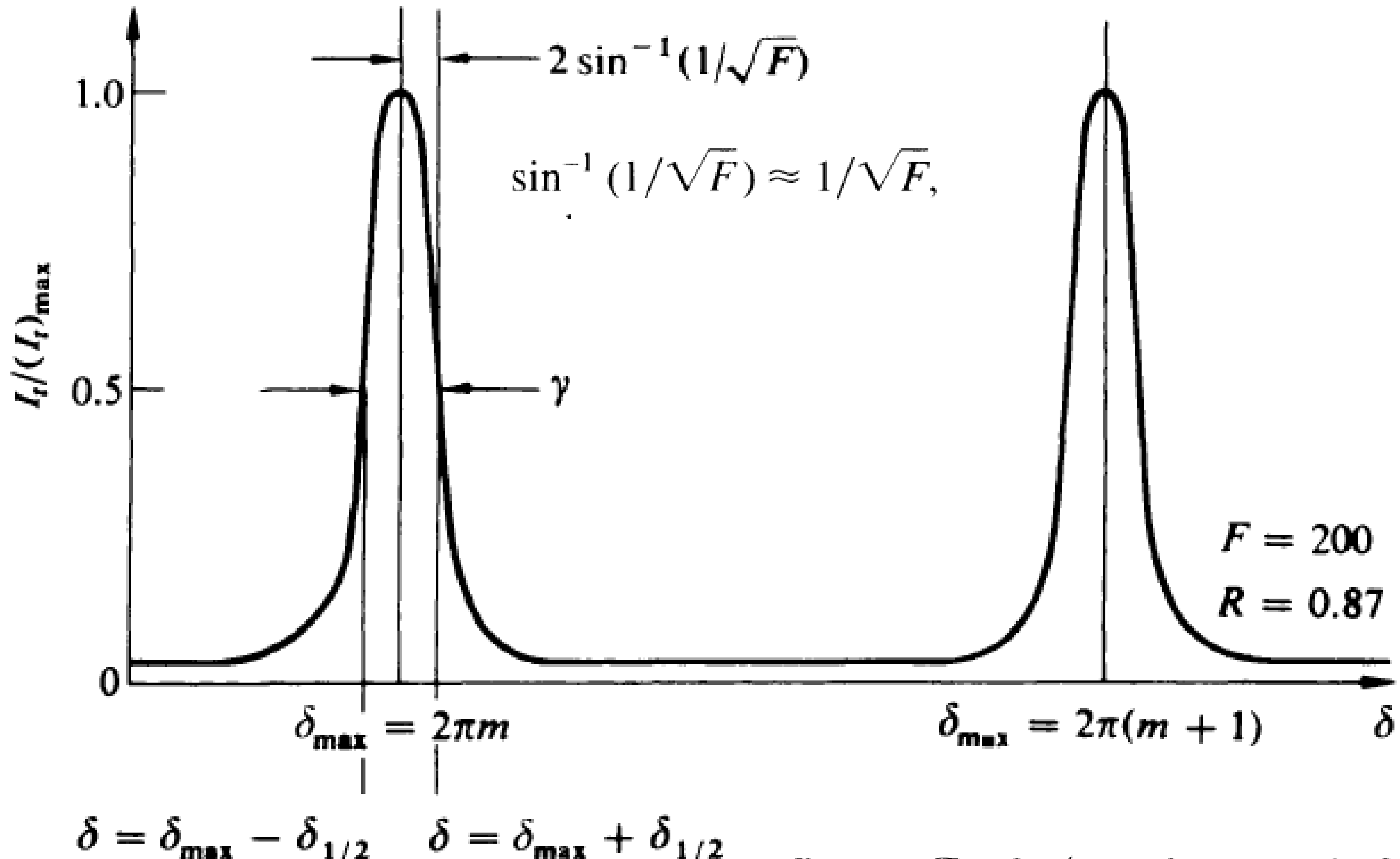

finesse, $\mathscr{F} \equiv 2\pi/\gamma$ or, from Eq. (9.69),

$$\mathscr{F} = \frac{\pi\sqrt{F}}{2}$$

Figure 9.45 Fabry–Perot fringes.